Experimental investigations on prototype heat storage units utilizing stable supercooling of sodium acetate trihydrate mixtures

Dannemand, Mark; Dragsted, Janne; Fan, Jianhua; Johansen, Jakob Berg; Kong, Weiqiang; Furbo, Simon

Published in:
Applied Energy

Link to article, DOI:
10.1016/j.apenergy.2016.02.038

Publication date:
2016

Document Version
Peer reviewed version

Title: Experimental investigations on prototype heat storage units utilizing stable supercooling of sodium acetate trihydrate mixtures

Authors: Mark Dannemand, Janne Dragsted, Jianhua Fan, Jakob Berg Johansen, Weiqiang Kong, Simon Furbo

Corresponding email: markd@byg.dtu.dk

Affiliation: Department of Civil Engineering, Technical University of Denmark, Brovej 118, Kgs. Lyngby, DK 2800, Denmark

Keywords: compact thermal energy storage; seasonal heat storage; supercooling; sodium acetate trihydrate; phase change material

Abstract

Laboratory tests of two heat storage units based on the principle of stable supercooling of sodium acetate trihydrate (SAT) mixtures were carried out. One unit was filled with 199.5 kg of SAT with 9% extra water to avoid phase separation of the incongruently melting salt hydrate. The other unit was filled with 220 kg SAT mixture thickened with 1% carboxymethyl cellulose. The heat exchange capacity rate during the charging of the unit with the extra water was significantly higher than for the unit with the thickening agent due to the different levels of convection. The SAT mixtures in the units were stable and supercooled at indoor ambient temperatures for up to two months, after which the units were discharged. The energy discharged after solidification of the supercooled SAT and water mixture was 194 kJ/kg in the first test cycle, dropping to 179 kJ/kg after 20 test cycles. The energy discharged from the unit with SAT and the thickening agent after solidification was stable at 205 kJ/kg over 6 test cycles.

1. Introduction

Heating of buildings and domestic hot water represent a large part of society's energy demand. Heating demands are especially high in winter. Solar energy is available all year round in most regions on earth, but it is limited in high-latitude regions in winter. It is more abundant in summer, when it can easily be harvested as low-grade thermal energy using solar collectors.

Thermal energy storage integrated in energy systems can help to optimize the use of energy resources by peak-shaving and making it possible to implement more renewable energy sources in our energy infrastructure [1]. This can lead to a reduction in greenhouse gas emissions from our thermal energy use and a reduction in environmental pollutants. Implementing more thermal energy storage may lead to more sustainable energy systems and may help to reduce climate change.

1.1 State of the art

Short-term storage of solar thermal energy for space heating and domestic hot water is typically done in small water storages, where continuous heat loss limits the storage period. With very large water storages, it is possible to store enough thermal energy to heat a single-family house during a winter. Alternatively, a form of thermal energy storage without continuous heat losses would allow for a more compact storage, where thermal energy could be stored from summer to winter in a seasonal heat storage. Large water storages for centralized systems are based on a relativity mature technology. Bauer et al. reported on various types of seasonal sensible heat storages

for central solar heating plants in Germany [2], and Novo et al. did a review seasonal heat storage in large water tanks and pits for centralized heating systems [3]. In both cases, the authors find the use of large sensible heat storage units feasible in centralized heating systems. On the smaller scale of individual buildings, Colclough and McGrath made a life cycle analysis of a low-energy single-family house with a solar combi system with a 23 m^3 water seasonal thermal energy storage [4]. They found that implementing seasonal heat storage in the combi system would reduce the carbon emissions and life cycle energy consumption of the system in the long term. Persson and Westermark looked at the financial aspect of seasonal thermal energy storages for individual houses and found that more competitive investment and annual costs could be offered if they were applied to passive houses [5]. Xu et al. did a review on available technologies for seasonal heat storage and reported that sensible heat storage technology has been implemented in many large-scale plants [6]. Their review also covered latent heat and chemical storages, which are still at the stage of material investigations and lab-scale experiments. Pinel et al. reviewed methods for seasonal storage of solar heat in residential applications, mainly focusing on sensible heat storages [7]. Their paper also mentions chemical and latent thermal energy storage principles. These technologies could be used to store thermal energy over longer periods in more compact systems, but they need further development. Yan et al. have reviewed promising candidate reactions for chemical heat storage [8], and Aydin et al. have reviewed thermochemical heat storage systems, including comparison with other storage methods. Both reviews conclude that the chemical storage principle is a promising technology, but needs further development before it can reach the market. Zondag et al. reported on the development of a small-scale prototype thermochemical heat storage system [9], and Mette et al. presented a solar thermal combi system with a thermochemical energy storage for long-term heat storage [10]. Both these reports demonstrate the storage principles, although they need more research.

1.2 Phase change material heat storage

Storages that use the latent heat of fusion of a phase change material (PCM) have been suggested by many authors for improving performance compared to sensible heat storages. Nkwetta et al. carried out numerical investigations on incorporating PCM in water tanks and found that it could increase the energy stored [11]. López-Navarro et al. did experimental investigations on a storage tank with PCMs and made a full experimental characterisation of its performance [12]. Nkwetta and Haghighat [13] and Sharif et al. [14] have written reviews on thermal energy storages with PCMs. None of these authors report using the supercooling of a PCM for long-term heat storage. In fact, the supercooling of a PCM in a latent heat storage has usually been seen as an undesirable effect that needs be avoided by using various nucleation agents. This is because it prevents the heat of fusion from being released as desired during the discharge process when the melting point of the PCM is reached [15]. However, when a PCM is in a supercooled state in temperature equilibrium with the ambient, the melting enthalpy of the PCM is stored, but no continuous heat loss occurs, which makes long-term heat storage possible. Sandnes and Rekstad carried out laboratory investigations on the stored enthalpy in small samples of supercooled salt hydrates [16], but do not report investigations of constructed storage units. Dannemand et al. have previously reported a number of barriers and solutions for the reliable operation of a storage unit utilizing the principle of stable supercooling of sodium acetate trihydrate (SAT) mixtures and elucidated the theoretical storage potential with numerical calculations [17], but they did not investigate the actual measured performance of storage units. One of the problems they list is the phase separation of the SAT. In another article, Dannemand et al. investigated the performance of a prototype unit containing a SAT mixture with extra water. The extra water was added to solve the phase separation problem. They focused on cycling stability, discharge power and discharge temperatures [18], but they did not explore the heat exchange capacity rate. Another way of avoiding~~to avoid~~ phase separation is to add a thickening agent to the SAT. This has been investigated ~~be~~ by several authors in small sample sizes [19–22]. However, t~~T~~he performance of SAT mixtures with thickening agents actively being used for ~~utilizing~~ supercooling in large application-~~-~~size heat storage units has not previously been reported.

1.3 Scope

This article reports on laboratory tests of two full-scale heat storage units for building heating purposes that use the principle of stable supercooling with two different PCM mixtures. The performance of a unit with a SAT mixture with extra water was compared with the performance a unit with a SAT mixture with carboxymethyl cellulose (CMC) – a thickening agent for avoiding phase separation. The experiments showed that the storage principle works in full-scale application-size units and that the unit with the SAT mixture with CMC as a thickening agent performed best. The heat exchange capacity rate of the heat storage prototypes, which is an important factor in system performance, was measured and compared. We also measured the energy released after the solidification of the supercooled PCMs, the discharge temperatures after solidification of the supercooled PCMs, and the cycling stability of the two units. The results verify the functionality of the storage concept in real application-size units and give an indication of the performance that can be expected from the first prototype storage units.

2. Experimental setup

The primary storage medium in the prototypes tested was sodium acetate trihydrate (SAT), which has a melting point of 58 °C and a latent heat of fusion of 264 kJ/kg [23]. It has been shown to supercool consistently down to temperatures well below 0 °C [24]. SAT is an incongruently melting salt hydrate and suffers from phase separation, especially over repeated heating and cooling cycles, where segregated anhydrous sodium acetate settles to the bottom of the PCM container and the water concentration in the upper part increases due to the density differences. When a PCM sample suffering from phase separation solidifies, not all possible trihydrate crystals will be formed because of the physical separation of water molecules in the upper part of the sample and segregated anhydrous sodium acetate in the lower part. This will reduce the effective latent heat of fusion of the bulk PCM and thereby also its storage capacity [25]. One solution that has been proposed is to add extra water to the salt hydrate so that the salt water mixture composition is always at a point where all salt is dissolved in the water when it is in supercooled liquid phase [26]. This requires soft mixing of the salt water mixture to avoid phase separation and reduces the energy density of the storage [27]. Another proposed solution for avoiding phase separation is to add a thickening agent to the PCM mixture. A suitable thickening agent will keep segregated anhydrous sodium acetate from settling to the bottom and keep the anhydrous salt suspended in the solution near the water it can recombine with at solidification.

2.1 PCM mixtures and material properties

A sodium acetate water mixture was prepared by melting the solid SAT in a closed barrel in a large oven for several days. To increase the water weight content from 39.7% of the SAT composition to 44.8% water and 55.2% sodium acetate, 9 wt% extra water was added. The other PCM was a mixture of SAT with 1% carboxymethyl cellulose (CMC) which was prepared by initially melting the SAT and then, with the SAT in a hot melted state, mixing in the CMC little by little, while mechanically stirring to ensure a uniform PCM mixture. CMC was chosen as the thickening agent due to the positive experience of several authors [19][20][21][22]. The ratio of CMC and SAT chosen was based on recommendations from the supplier of the additive. A series of tests with smaller sample sizes showed that 1% CMC was the minimum quantity for a stable uniform mixture.

The specific heat capacities for the solid and liquid phases and the latent heat of fusion of the PCM mixtures were determined using the findings of Araki [28]. Non-temperature-dependent specific heat capacities for the solid and liquid phase PCM mixtures were determined as the average over the relevant temperature intervals. The properties for the SAT and 1% CMC mixture were estimated to be the same as for SAT without extra water in Araki's findings. The value for the latent heat of fusion of SAT without extra water determined by Araki's correlation is slightly lower than the values generally stated in the literature [23]. Material properties applied for theoretical calculations are listed in Table 1.

Table 1. Thermal properties of the PCM mixtures.

Material property	SAT + 9% H_2O	SAT + 1% CMC
Solid specific heat c_p(s)	2.2 kJ/kgK	2.1 kJ/kgK
Liquid specific heat c_p(l)	3.1 kJ/kgK	3.0 kJ/kgK
Latent heat of fusion L	189.4 kJ/kg	250 kJ/kg

2.2 Heat storage units

The units were designed as flat rectangular chambers for the PCM with an internal height of 50 mm. The low height was to reduce the risk of phase separation. The width and length of the units were 1200 x 2400 mm. One unit was made from normal steel and the other had the inner chamber for the PCM made in stainless steel. Steel and stainless steel in combination with SAT have been shown to be stable over long periods with regard to corrosion and chemical reactions [29],[30]. At one end of the units were 300 mm wide and 100 mm high extensions in the width of the units. These were incorporated to allow for expansion of the PCM mixture during heating. The units had separate heat exchangers at the top and bottom of the PCM chamber. The heat exchangers had manifolds along the sides of the units. Each manifold had a cross section of 30 x 30 mm. The bottom surface of the PCM chamber was covered by 16 parallel channels and 14 channels covered the top surface. The heat exchangers were incorporated on to the outer surfaces of the PCM chamber to transfer heat through the top and bottom surfaces of the PCM chamber, as shown in Figure 1 and Figure 2. This enabled the PCM to be heated to a relatively uniform temperature to obtain complete melting of all crystals. It also allowed mixing of the salt water mixture by convection during heating. The internal height of the heat exchanger channels was 4 mm and the width was 130 mm separated by 20 mm spacers. The internal volumes of the chambers were approximately 144 litres for the PCM and another 30 litres for the expansion volume. No heat exchangers were incorporated on top of the expansion volume. The thickness of the steel plates was 2 mm. The mass of each empty unit was 236 kg. The total volume of heat transfer fluid (water) in the heat exchangers including the manifolds was 32 litres in each unit.

When rigid constructions such as steel are used, the density change between the cold solid and the warm liquid salt can cause pressure changes and deformations of the tank. Just as bending a metal disk with cracks work as a triggering mechanism for pocket-sized heat packs [31], small cracks on the inside of the PCM chamber can in combination with pressure changes and deformations work as an uncontrolled activation mechanism, e.g. at joints or welds. To reduce the pressure changes in the PCM chamber during heating and cooling, an inflatable plastic bag or an expansion vessel without pre-pressure was connected to the expansion volume via a tube to allow for expansion of the PCM mixture without pressure build-up inside the PCM chamber. This closed design made it possible to heat the salt hydrate to a high temperature without loss of water vapour from the PCM. Moreover, the metastable state of the supercooled salt hydrate is easily interrupted by external disturbances, so a closed container is naturally more stable.

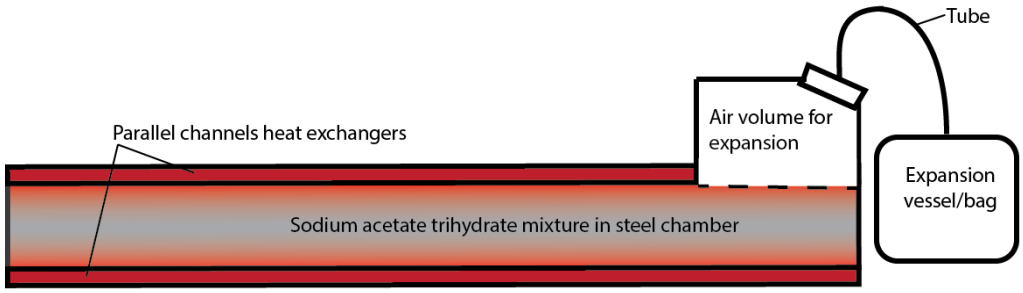

Figure 1. Diagram of unit with PCM chamber, heat exchangers on top and bottom surfaces, and integrated and external expansion.

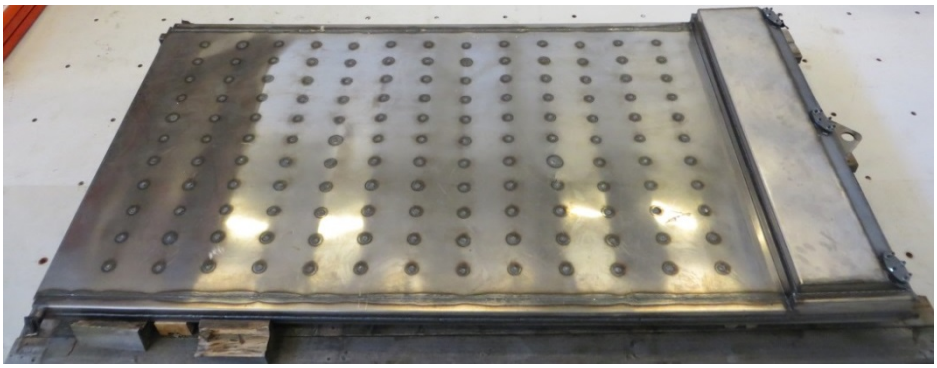

Figure 2. 1200 x 2400 x 60 mm unit with heat exchangers on the top and bottom surfaces, and integrated expansion volume.

The inner surfaces of the PCM chamber were designed and manufactured to be simple and smooth without cracks or gaps. This was to avoid spontaneous nucleation caused by possible movement of cracks. Thirty pipe segments of 50 mm length were welded inside the PCM chamber to the top and bottom surfaces functioning as supports and to provide the unit with a rigid construction. One support inside the PCM chamber can be seen in Figure 3.

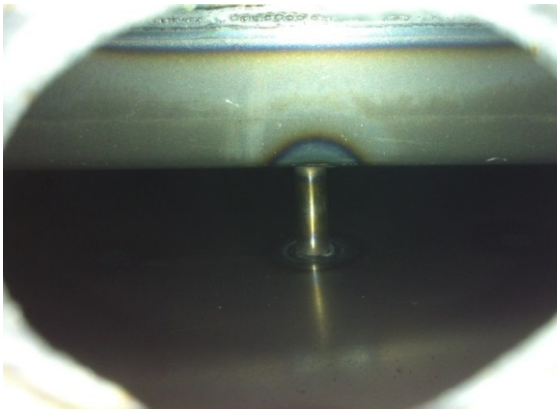

Figure 3 View of a round stabilizer through filling neck

Three openings to the PCM chamber were provided for filling the chamber with PCM and for installing the tube for the expansion tank and a probe to measure the temperature of the PCM. These filling necks were closed with lids and 3 mm thick rubber gaskets, as shown in Figure 4. The filling necks were located in the upper part of the expansion volume to avoid contact between the PCM and the lids and gaskets.

Figure 4. Expansion volume with filling necks, rubber gaskets and lids.

2.3 Activation of solidification

Crystallization and the release of the heat of fusion from the supercooled SAT initiate when the first seed crystal of a certain size appears in the solution. After that, the crystallization will spread to the entire volume and the temperature will rise approximately to the melting point of the PCM. It has been shown that cooling a supercooled SAT mixture to a low temperature eventually causes crystallization of the supercooled solution [32]. To utilize this

cooling technique to initiate the crystallization of the supercooled PCM, a 100 ml chamber was welded to the outside of each unit in good thermal contact with the PCM chamber at the opposite end to the expansion volume, as shown in Figure 5. Liquid CO_2 with a pressure of 5-6 bars could then be flushed through this chamber to cool a small part of the PCM through the chamber wall to a low temperature as the CO_2 evaporated, and thus initiate nucleation.

Figure 5. CO_2 chamber for activating solidification of supercooled PCM mixture by cooling.

2.4 Filling

The units were filled with the melted PCM mixture at a temperature of approximately 80 °C in a slightly tilted position to achieve complete filling of the PCM chamber. The unit was filled until the level of PCM was 2-4 cm higher in the expansion volume than elsewhere in the unit. This would allow for some contraction of the PCM during solidification while keeping a height of 5 cm in solid state at 25 °C in the entire unit, if the crystallization occurred homogeneously without air pockets in the PCM chamber.

Being handmade, the geometry of the units differed somewhat. The densities of the PCM mixtures also differed slightly due to different additives, which meant the units ended up containing different PCM masses. The steel unit contained 199.5 kg of SAT with 9% extra water (44.8 wt% water and 55.2 wt% sodium acetate). The unit with the inner chamber in stainless steel contained 220 kg of SAT thickened with 1% CMC. During testing the units were supported on a bed of 100 mm insulating material and a layer of 100 mm insulation was placed on the top and around the sides of each unit. An overview of the two units is given in Table 2.

Table 2. Unit chamber material and PCM mixture and masses.

	Unit 1	Unit 2
PCM mixture	SAT + 9% H_20	SAT + 1% CMC
PCM mass	199.5 kg	220 kg
PCM chamber material	Steel	Stainless steel

Copper/constantan thermocouples were used to measure the surface temperature of the units on the outside of the heat exchangers, at the front and back of each unit, near the lids, and at the CO_2 chamber. One thermocouple in a probe was inserted through one of the filling necks to measure the temperature of the PCM. Thermopiles were used to measure the temperature difference across the inlets and outlets of the heat exchangers. Two Brunata HGQ1 flow meters were used to measure the flow rate to the heat exchangers. Solartron cards were used with a PC to record data every 10 seconds.

3. Test procedure and calculations

The units were connected to a heat storage test facility so that they could be heated and cooled under controlled conditions. Twenty test cycles with different flow rates, charge and discharge powers, temperatures settings and durations were carried out with the unit with extra water. Six test cycles were carried out with the unit containing SAT and CMC.

To achieve supercooling of the SAT mixture, it is necessary that all crystals of the bulk PCM are melted, so that the PCM will not crystallise when it cools down. There appears to be a link between the level of heating above the melting point and the stability of the supercooling, as reported by Wei [33]. Our initial investigations showed that a temperature of at least 20 K above melting point in the entire volume helped to achieve stable supercooling.

The power of the heating element used for charging the units in the test facility was 6-9 kW. The units were charged for a period of 10-22 hours with an inlet temperature of 90-94 °C and a flow rate of 10-11 l/min in each heat exchanger. Inlet, outlet and storage temperatures were typically stable after approximately 8 hours of charging. After a stable hot period, the units were discharged with the aim of achieving a supercooled state with a flow rate of 2 l/min in each heat exchanger and an inlet temperature of approximately 25 °C. This temperature could represent the return temperature of a low-temperature heating system. The heat sink was the central cooling system of the test facility connected via a heat exchanger and controlled by a thermostatic valve. The response time of the valve caused the discharge temperature to vary somewhat throughout the discharge period. In some tests the aim was to keep the PCM stable in a supercooled state over a long period. In these tests, the units passively cooled towards the ambient temperature and were not actively discharged.

After the PCM had remained in a supercooled state for a period of time, crystallization was started by flushing CO_2 through the CO_2 chamber to cool a small part of the PCM. The energy released after solidification was discharged with a flow rate of 2 l/min in each heat exchanger.

The charge and discharge powers of the storage unit were determined by:

$$\dot{Q}_{charge} = \dot{V} \cdot c_p \cdot \rho \cdot (T_{in} - T_{out}) \qquad \text{Equation 1}$$

where $\dot{V}$ is the volume flow rate of the heat transfer fluid measured at the inlet, T_{in} is the inlet temperature, T_{out} is the outlet temperature, c_p is the specific heat capacity of the heat transfer fluid at mean temperature between T_{in} and T_{out}, and ρ is the density of the heat transfer fluid at T_{in}.

The heat loss coefficient of the storage unit was determined by heating the unit to a stable temperature over a long period. The energy balance of the system was used to determine the heat loss experimentally. The energy added to the system was equal to the heat loss when the storage temperature remained stable over a period. In this way a heat loss coefficient with a constant value could be determined for the specific temperatures by:

$$H_{loss} = \dot{Q}_{charge} / (T_s - T_{amb}) \qquad \text{Equation 2}$$

where T_s is the average surface temperature of the unit in a stable hot period, and T_{amb} is the ambient temperature. The heat loss coefficient for the storage unit was used to calculate the energy content of the storage unit based on the measured data.

The change of heat content in the unit over a specific time period during a charge was determined by:

$$E_{charge,measured} = \int_0^{t_c} \left[\dot{Q}_{charge} - H_{loss} \cdot (T_s - T_{amb}) \right] dt \qquad \text{Equation 3}$$

where T_s is the average surface temperature of the unit in the relevant time step, and t_c is the duration of the charge period. A similar procedure was used to determine discharged energy.

The heat exchange capacity rate (HXCR) expresses the ability to transfer thermal energy from a heat transfer fluid to the PCM material in the storage unit. It depends on the design of the heat exchanger of the storage unit, the operating conditions, and the thermophysical properties of the PCM. The HXCR is derived from the heat transfer rate and the log mean temperature difference [34], [35]:

$$HXCR = \dot{V} \cdot c_P \cdot \rho \cdot ln\left(\frac{T_{in} - T_{PCM}}{T_{out} - T_{PCM}}\right) \qquad \text{Equation 4}$$

where T_{PCM} is the PCM temperature measured by the probe inserted in the PCM. A high HXCR is desirable, so that the storage unit can be charged fast, e.g. when solar thermal energy is available, and so that it can be discharged with sufficient power to meet a given demand.

Finally, the measured heat per unit mass of PCM released after solidification of the supercooled PCM was determined for the test cycles to evaluate its cycling stability and storage potential, and to compare the two different PCMs.

With a specific heat of steel of 500 J/kgK and 32 litres of water in the heat exchangers, the theoretical heat capacity C_{unit} of the storage unit was determined to be 252 kJ/K.

3.1 Theoretical calculations

The measured thermal energy charged to and discharged from the storage units was compared to the theoretical energy content calculated by Dannemand et al. [17] for a PCM storage with stable supercooling taking into account the latent heat of fusion, the specific heat capacities of the solid and liquid PCM, and the sensible heat of the storage tank material and heat transfer fluid. Their theoretical model indicates that the energy released from supercooled SAT at ambient temperature will be lower than the latent heat of fusion at the melting point, because the specific heat of the supercooled SAT is higher than the specific heat of the solid SAT. Their model also assumes that the PCM behaves like an ideal compound, which changes phase from solid to liquid at a specific melting temperature. When extra water is added to salt hydrates, phase change happens over a temperature range [26]. In our investigations, the focus was on the differences in energy content between the initial, the fully heated, the supercooled, and the discharged conditions. The simple theory with a specific melting temperature therefore provides a sufficient basis for comparison.

These sets of formulae were applied when calculating the theoretical energy content of the storage units with different start, maximum, supercooled and end temperatures, so that the measured values could be compared to theoretical values over the same temperature intervals.

4. Results and Discussion

4.1 Test cycle energy content

The following section summarizes the results for the 13th test cycle of the unit with SAT and extra water. The 13th test cycle was typical for the test series. From a starting temperature of 24.6 °C, the unit was charged with a flow rate of 21 l/min for both heat exchangers combined. Stable conditions with an average heat storage temperature of 90.1 °C were reached after approximately 8 hours of charging. The heat loss coefficient was experimentally determined using Equation 2 to be H_{loss} = 8 W/K at 90 °C over a 12-hour period.

The total energy stored in the unit, including PCM mixture and steel, for this temperature interval was 91.4 MJ, calculated from Equation 3. The accumulated heat loss from this 8-hour charge period was 10.8 MJ. Figure 6 shows the accumulated heat loss over time, the energy stored in the unit, the total energy charged into the unit including the heat loss, and the PCM temperature during the test cycle. This illustrates the energy content of the unit during the test cycle and the different stages of the cycle.

The theoretical thermal energy change in the unit for this temperature set and for the material properties in Table 1 was calculated to be 88.7 MJ. The measured energy content was 3% higher than the theoretical energy content. The measured energy discharged from the stable hot state to the supercooled state was 58.2 MJ. This is 5% higher than the theoretical discharged energy of 55.3 MJ.

After the unit had remained in supercooled state for three days at a storage temperature of 26.4 °C, the crystallization was started using the CO_2 cooling technique. The temperature on the outside of the CO_2 container reached −34 °C before the activation was registered as a temperature increase on a nearby thermocouple. The unit was discharged with a flow rate of 2 l/min in each heat exchanger to a temperature of 24.8 °C. After eight hours, all surface temperature sensors had stabilized and the unit was fully discharged. The total thermal energy discharged 8

hours after solidification was 35.7 MJ. The theoretical thermal energy discharged for this temperature set and properties of SAT with 9% extra water listed in Table 1 was 33.2 MJ. So, the measured energy discharged after solidification of the supercooled sodium acetate water mixture was 7.5% higher than the theoretical.

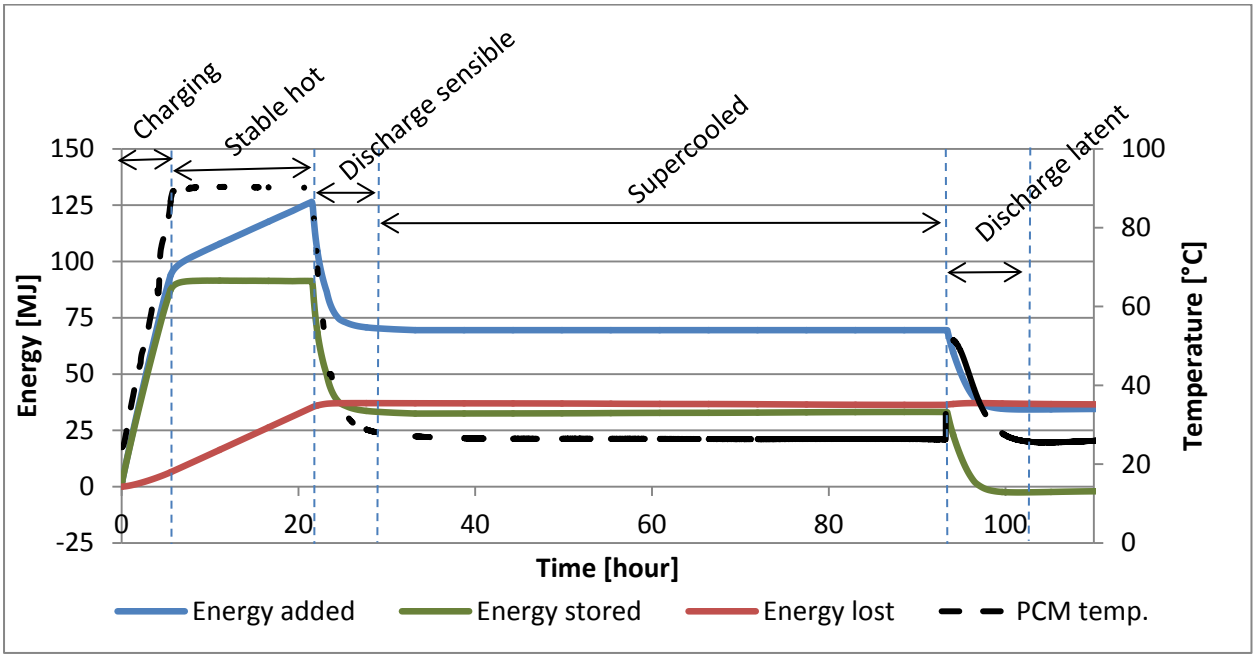

Figure 6. Energy content of unit with SAT and extra water, accumulated heat loss and total energy added during a test cycle.

Table 3 gives a summary of charge, discharge and solidification energies for the test cycle with SAT and extra water and for a test cycle with SAT and 1% CMC, along with the respective temperature intervals.

Table 3. Energy content of PCM in units during charge, discharge and activation.

	199.5 kg SAT with 9% extra water			220 kg SAT with 1% CMC		
	Temperature range	Theoretical	Measured	Temperature range	Theoretical	Measured
Charge	24.6 °C – 90.2 °C	88.7 MJ	91.4 MJ	26.1 °C – 92.5 °C	109.1 MJ	108 MJ
Discharge	90.2 °C – 26.4 °C	55.3 MJ	58.2 MJ	92.5 °C – 26.2 °C	60.4 MJ	59.8 MJ
Solidification	26.4 °C – 24.8 °C	33.2 MJ	35.7 MJ	23.6 °C – 24.2 °C	47.8 MJ	45.2 MJ

The deviation between the theoretical energy content and the measured values could indicate that incorrect values were used for the PCM properties in the theoretical calculations. A value for the latent heat of fusion of 202 kJ/kg instead of 189.4 kJ/kg for the SAT-water mixture, and of 242 kJ/kg instead of 250 kJ/kg for the SAT-CMC mixture would minimize deviations between the theoretical calculations and measured values.

4.2 Cycling stability

With a temperature of the supercooled storage and a final discharge temperature of approximately 25 °C, the energy released after solidification of the supercooled SAT with extra water in the first test cycle was 194 kJ/kg of PCM. In the 5th test cycle, 188 kJ/kg was discharged. After 20 test cycles, the measured discharged energy was 179 kJ/kg of PCM. This indicates that the problem of phase separation was not completely solved by adding 9% extra water, because the discharged energy declined over the test cycles. Mixtures with larger water content may show better cycling stability.

The energy released from the supercooled PCM in the unit with 1% CMC was consistently around 205 kJ/kg of PCM over the six test cycles.

In one test cycle, the unit with SAT and extra water was kept in supercooled state for eight weeks, while the unit with thickening agent was kept in supercooled state for five weeks before solidification was activated by cooling with CO_2. There was no significant difference in the energy discharged after a short or a long storage period.

In 13 of the 20 test cycles with the unit with SAT and extra water, the crystallization started spontaneously during discharge. In some tests, this was probably due to too low temperatures in the SAT caused by too short charge periods. In later test cycles, the PCM solidified spontaneously in three consecutive test cycles, after which the expansion bag was dismounted and it was observed that the tube between the unit and the expansion bag had been blocked with SAT. After cleaning the tube and remounting the expansion vessel, stable supercooling was again achieved. This indicates that the solution to the problem of the expansion of the PCM using a tube connected to an external expansion vessel may not be durable in the long run. In the unit with SAT and CMC, the crystallization started spontaneously in two of the six test cycles. In the remaining test cycles, the solidification was triggered by cooling with CO_2 after the PCM had remained supercooled and stable at ambient temperatures.

4.3 Heat exchange capacity rate

Figure 7 shows the heat exchange capacity rates for the top and bottom heat exchangers for selected charges with similar test conditions for the two units. The HXCR for the unit with extra water increased during the charging period and the HXCR for the unit with thickening agent decreased until the end of the charge period. Sudden increases in HXCR occurred after 4 hours for the unit with SAT and extra water and after 6 hours for the unit with SAT and CMC. This was when the PCMs were fully melted and convection could occur throughout the respective PCM chambers. The HXCR was higher for the bottom heat exchanger in both units, partly because of the larger surface area of bottom heat exchanger and partly because heating the PCM from the bottom induced convection in the melted PCM, while heating from the top did not. The main reason for the difference in HXCR between the two units was the different levels of convection in the two PCM mixtures. The melted SAT with water mixture had a lower viscosity and therefore more convection occurred than in the melted SAT mixture with CMC, where convection remained low even after melting due to its higher viscosity. Sun et al. also report that the convection in PCM has a significant effect on the heat transfer in a PCM storage [36].

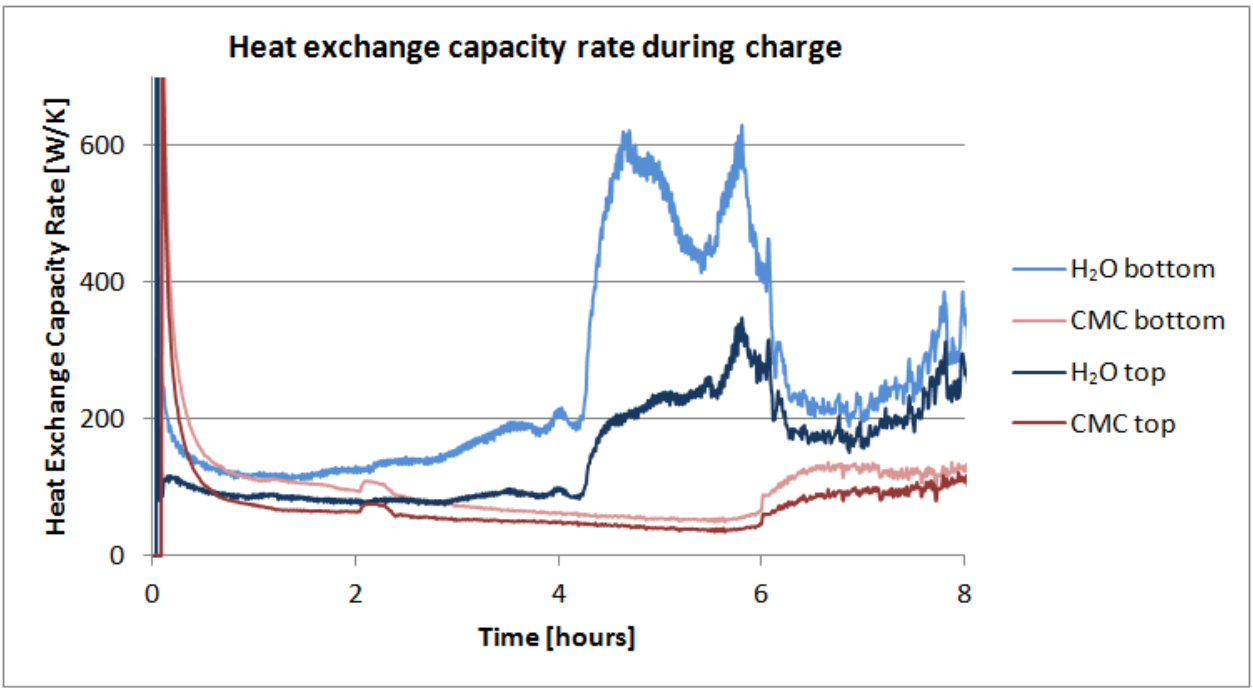

Figure 7. Heat exchange capacity rate during charging for top and bottom heat exchangers for units with PCM mixtures with extra water and CMC.

Another factor that affects the HXCR of the exchangers is convection of the heat transfer fluid inside the heat exchangers, which in the case of charging enhances the heat transfer in the bottom heat exchangers.

After solidification of the supercooled PCMs and the following discharges, the HXCRs for the two units showed a similar tendency. At this time, both PCMs were in solid states and there was no convection in the PCMs. With a flow rate of 2 l/min, the HXCR started at 160-180 W/K and dropped during the discharge.

4.4 Solidification temperatures

Figure 8 and Figure 9 show the temperatures the PCMs reached after solidification from the supercooled state, the inlet and the outlet temperatures of the heat transfer fluid in the heat exchangers. The flow rates were 2 l/min in each heat exchanger. The maximum temperatures measured in the probes submerged in the PCMs after solidification were 53 °C for the SAT with extra water and 58 °C for the SAT with CMC. The higher outlet temperatures of the bottom heat exchangers were partially due to the larger area of the bottom heat exchangers. Another possible explanation could be non-optimal contact between the PCMs and the top heat exchangers caused by cavities or air bubbles formed during contraction of the PCMs as they cooled. The inlet temperatures during the discharge varied due to the response time of the thermostatic valve in the cooling loop.

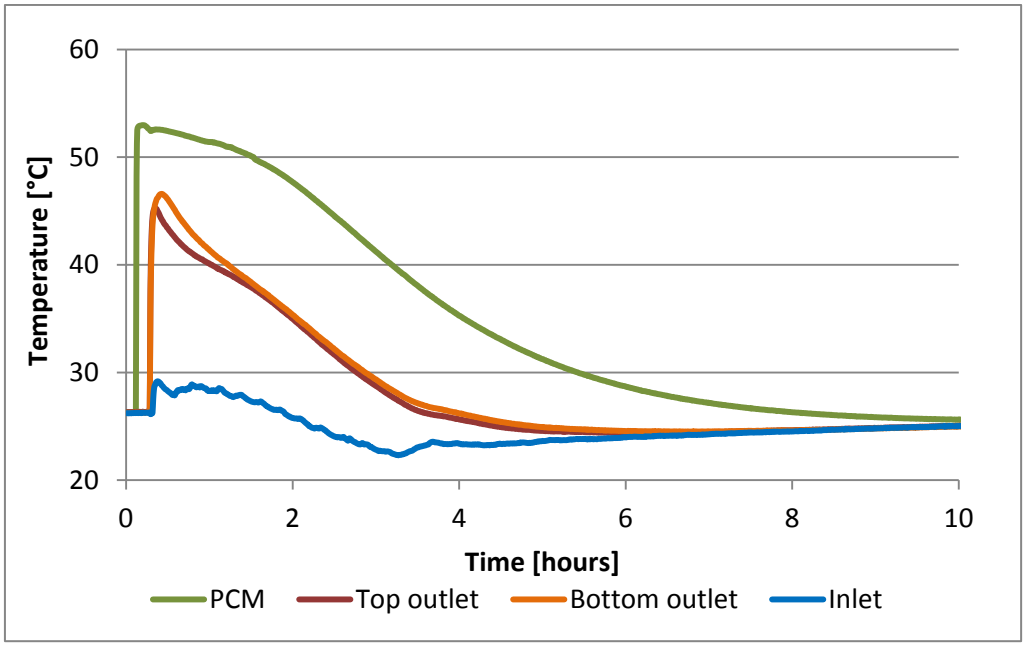

Figure 8. PCM, inlet, top outlet and bottom outlet temperatures for the unit with extra water.

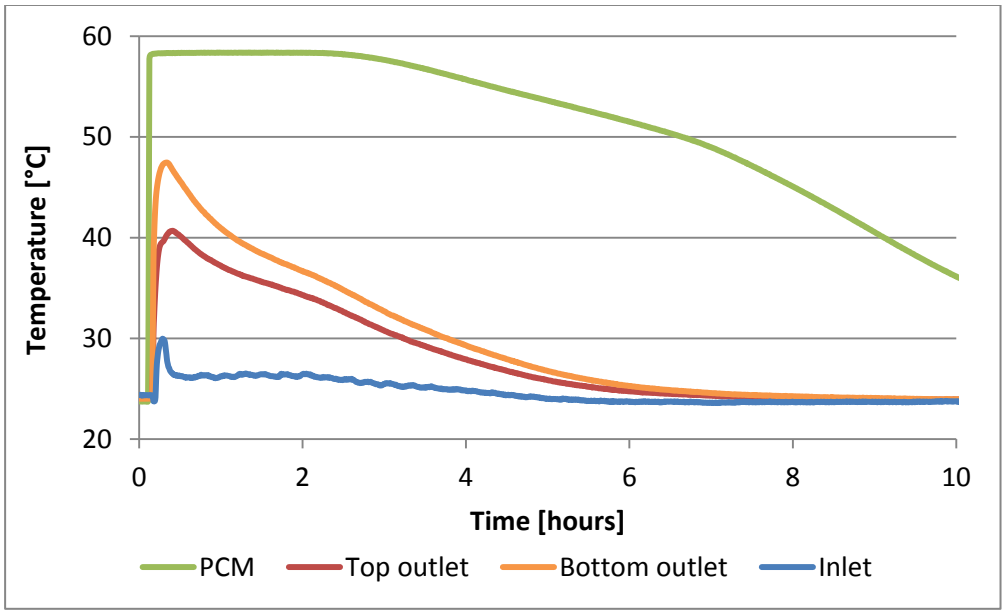

Figure 9. PCM, inlet, top outlet and bottom outlet temperatures for the unit with thickening agent.

A test with a discharge flow rate of 0.5 l/min increased the maximum average outlet temperature at the start of the discharge by 2-3 K.

4.5 Discharge power

The total discharge powers combining both top and bottom heat exchangers in each of the two units are shown in Figure 10. The unit with SAT and CMC contained 10% more PCM mixture with a higher latent heat of fusion. This unit could therefore be discharged with a higher power and for a longer duration than the unit with SAT with extra water. The difference was especially clear in the second half of the discharge period. Discharging with a lower flow rate led to a lower initial power peak, but a longer discharge period. The discharge flow of the unit with extra water started with a time delay after solidification of the supercooled PCM. In this case the water in the heat exchangers had more time to heat up before the flow started. This is the reason for the earlier peak in the discharge power for the unit with extra water in Figure 10.

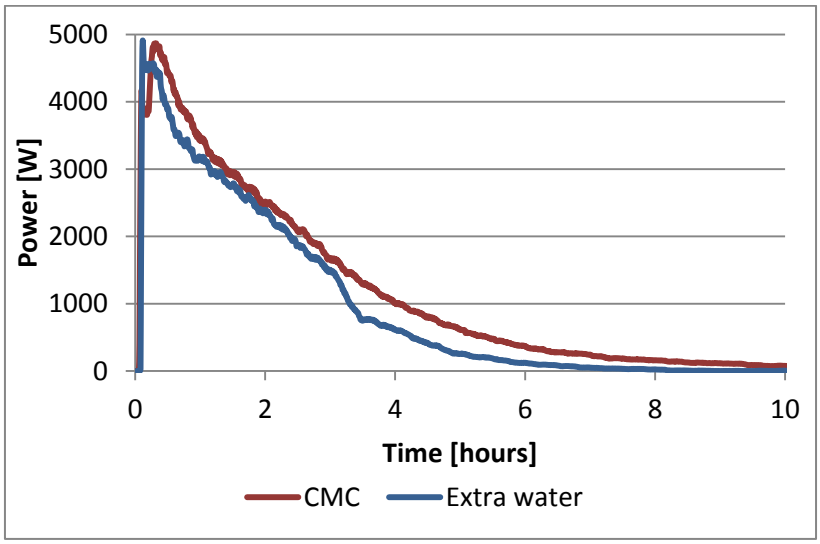

Figure 10. Total discharge powers for units with sodium acetate trihydrate with extra water and CMC.

4.6 Unit and heat exchanger design

A thermovision image of the top surface of one of the units is shown in Figure 11. The image was taken approximately 30 minutes after charging had begun. The inlet for the top heat exchanger was in the top left corner of the unit while the outlet is shown in the bottom right. The inlet manifold is on the left in the image and the outlet manifold is on the right. The flows in the channels across the top surface in the image are from left to right.

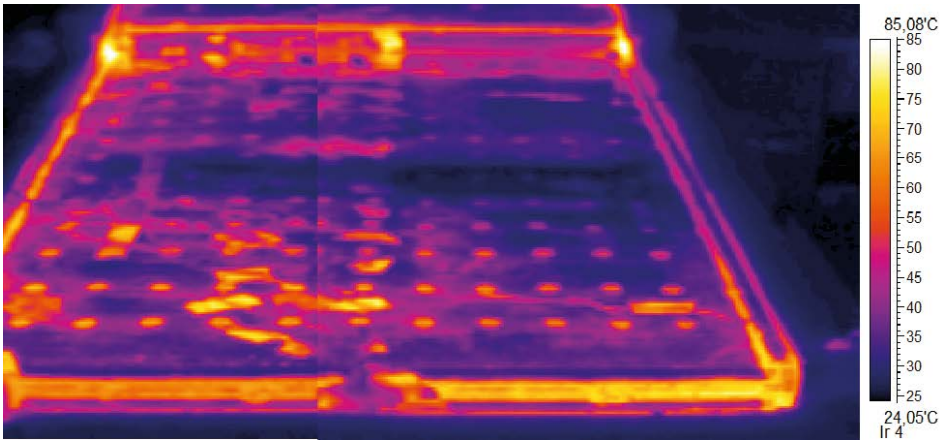

Figure 11. Thermovision image of the top surface of a unit during charging.

It can be seen from Figure 11 that the temperature on the top surface was not uniform. A cooler area in the central channels can be observed. This indicates that the flow distribution was not uniform across the channels. Applying the theory for flow distribution in Z-configured solar collectors, the uneven flow distribution could be due to too high pressure drops in the manifolds compared to the pressure drop in the individual channels [37]. If so, increasing the cross section area of the manifolds by a factor of 3 might give a more even flow distribution. With an even flow distribution in the heat exchanger channels, we would expect shorter charge times and higher discharge powers and temperatures. The PCM in the space immediately below the expansion volume is furthest away from the heat exchangers and will therefore be the area where the full melting and discharge happens last.

The laboratory testing also showed that it was difficult to flush out air trapped in the heat exchangers in this flat unit design. Furthermore, the flat rectangular design limited the possible operation pressure in the heat exchangers, which might not be compatible with the operation pressure elsewhere in a solar heating system.

For design development, it is therefore recommended that the heat exchangers should allow relatively uniform heating and discharge of the PCM for optimal performance. The design should also make it easy for any air in either the heat exchanger or the PCM chamber to escape. This would help ensure optimal heat transfer between the PCM and the heat transfer fluid. And a design with flexible expansion integrated in the unit instead of the external expansion vessel would be an improvement.

The phase separation problem of the SAT was solved with thickening agents in this flat unit, so it should be investigated whether taller units would also allow for a stable SAT composite throughout multiple charge and discharge cycles. Other thickening agents or other additives may also prove functional. Cylindrical unit designs and heat exchangers made of tubes may cope better with internal pressures than the flat unit design presented here. Tall cylindrical shaped units might also reduce the cost of manufacture compared to the flat design.

4.7 Integration of heat storage units in solar heating system

The laboratory investigations showed that it was possible to fully melt SAT mixtures and obtain stable supercooled PCMs ~~SAT mixtures~~ in 200 kg units ~~with 200 kg with~~using an inlet flow temperature of 90 °C. This temperature could be delivered by solar collectors. By placing a number of heat storage units in a utility room, e.g. in the basement of

the house, the heat to melt the SAT mixtures could be transferred from the solar collectors to the units by a piping system. In the laboratory tests, the discharge temperature and power after solidification was high enough to cover the requirements of a low-temperature heating system in a single-family house, e.g. a floor-heating system. The heat could ~~possibly~~ also be used for the preparation of domestic hot water. ~~Based on the heat demand of the house, t~~The number of units required ~~for covering~~to cover the heat ~~given~~ demand can easily be calculated. With this seasonal heat storage technique, the heating demand~~s~~ of a single-family house could theoretically be covered 100% by solar energy.

5. Conclusions

Experimental investigations have shown that it is possible to store thermal energy in supercooled sodium acetate trihydrate mixtures in units of a size that could be used for real applications. One prototype unit contained 199.5 kg of SAT with 9% extra water and was stable in supercooled state at ambient temperature for up to 2 months before solidification was intentionally started. Another unit contained 220 kg of SAT thickened with 1% carboxymethyl cellulose and was stable in supercooled state at ambient temperature up to 5 weeks before solidification was intentionally started. This shows that CMC works in large-scale applications.

The heat exchange capacity rate during charging of the unit with SAT and extra water was significantly higher than for the unit with SAT and CMC due to the higher viscosity of the thickened PCM. Initiating the crystallization of the supercooled PCM was done by cooling a small part of the SAT mixture to its maximum degree of supercooling by flushing pressurized liquid CO_2 through a small chamber attached to the outside of the PCM chamber. The energy discharged after solidification of the supercooled SAT with 9% extra water was 194 kJ/kg of PCM in the first cycle, 188 kJ/kg after five test cycles and 179 kJ/kg after 20 test cycles. The energy discharged after solidification of the SAT with CMC was stable at around 205 kJ/kg of PCM over six test cycles. The SAT with extra water reached 53 °C after solidification and the SAT mixture with CMC reached 58 °C after solidification. For both PCMs the outlet temperature reached approximately 45 °C at the beginning of the discharge with a flow rate of 2 l/min in each heat exchanger. The discharge power after solidification of the supercooled PCMs peaked at 4.5 – 5 kW at the beginning of the discharge and remained above 1 kW for approximately 4 hours. Crystallization of the PCM mixtures happened spontaneously in some test cycles and stable supercooling was not always achieved.

Acknowledgements

This project was funded by the European Commission as part of the Seventh Framework Programme of the European Community for Research, Technological Development and Demonstration Activities under the funding scheme of “Collaborative Project” through the COMTES consortium, Grant Agreement N° 295568. We thank our partner Henry Sørensen from Nilan A/S for constructing the storage unit prototypes and our partners Hermann Schranzhofer and Christoph Moser from Graz University of Technology for discussions and sharing their knowledge. We thank our technicians Martin Dandanell and Claus Aagaard for constructing the test rig for the units.

References

[1] L.F. Cabeza, L. Miró, E. Oró, A. de Gracia, V. Martin, A. Krönauer, et al., CO2 mitigation accounting for Thermal Energy Storage (TES) case studies, Appl. Energy. 155 (2015) 365–377. doi:10.1016/j.apenergy.2015.05.121.

[2] D. Bauer, R. Marx, J. Nußbicker-Lux, F. Ochs, W. Heidemann, H. Müller-Steinhagen, German central solar heating plants with seasonal heat storage, Sol. Energy. 84 (2010) 612–623. doi:10.1016/j.solener.2009.05.013.

[3] A. V. Novo, J.R. Bayon, D. Castro-Fresno, J. Rodriguez-Hernandez, Review of seasonal heat storage in large basins: Water tanks and gravel-water pits, Appl. Energy. 87 (2010) 390–397.

444 doi:10.1016/j.apenergy.2009.06.033.

445 [4] S. Colclough, T. McGrath, Net energy analysis of a solar combi system with Seasonal Thermal Energy Store,
446 Appl. Energy. 147 (2015) 611–616. doi:10.1016/j.apenergy.2015.02.088.

447 [5] J. Persson, M. Westermark, Low-energy buildings and seasonal thermal energy storages from a behavioral
448 economics perspective, Appl. Energy. 112 (2013) 975–980. doi:10.1016/j.apenergy.2013.03.047.

449 [6] J. Xu, R.Z. Wang, Y. Li, A review of available technologies for seasonal thermal energy storage, Sol. Energy.
450 103 (2013) 610–638. doi:10.1016/j.solener.2013.06.006.

451 [7] P. Pinel, C. a. Cruickshank, I. Beausoleil-Morrison, A. Wills, A review of available methods for seasonal
452 storage of solar thermal energy in residential applications, Renew. Sustain. Energy Rev. 15 (2011) 3341–
453 3359. doi:10.1016/j.rser.2011.04.013.

454 [8] T. Yan, R.Z. Wang, T.X. Li, L.W. Wang, I.T. Fred, A review of promising candidate reactions for chemical heat
455 storage, Renew. Sustain. Energy Rev. 43 (2015) 13–31. doi:10.1016/j.rser.2014.11.015.

456 [9] H. Zondag, B. Kikkert, S. Smeding, R. De Boer, M. Bakker, Prototype thermochemical heat storage with open
457 reactor system, Appl. Energy. 109 (2013) 360–365. doi:10.1016/j.apenergy.2013.01.082.

458 [10] B. Mette, H. Kerskes, H. Drück, H. Müller-Steinhagen, New highly efficient regeneration process for
459 thermochemical energy storage, Appl. Energy. 109 (2013) 352–359. doi:10.1016/j.apenergy.2013.01.087.

460 [11] D.N. Nkwetta, P.-E. Vouillamoz, F. Haghighat, M. El-Mankibi, A. Moreau, A. Daoud, Impact of phase change
461 materials types and positioning on hot water tank thermal performance: Using measured water demand
462 profile, Appl. Therm. Eng. 67 (2014) 460–468. doi:10.1016/j.applthermaleng.2014.03.051.

463 [12] A. López-navarro, J. Biosca-taronger, J.M. Corberán, C. Peñalosa, A. Lázaro, P. Dolado, et al., Performance
464 characterization of a PCM storage tank, Appl. Energy. 119 (2014) 151–162.
465 doi:10.1016/j.apenergy.2013.12.041.

466 [13] D.N. Nkwetta, F. Haghighat, Thermal energy storage with phase change material - A state-of-the art review,
467 Sustain. Cities Soc. 10 (2014) 87–100. doi:10.1016/j.scs.2013.05.007.

468 [14] M.K.A. Sharif, a a Al-abidi, S. Mat, K. Sopian, M.H. Ruslan, Review of the application of phase change
469 material for heating and domestic hot water systems, Renew. Sustain. Energy Rev. 42 (2015) 557–568.
470 doi:10.1016/j.rser.2014.09.034.

471 [15] J. Guion, M. Teisseire, Nucleation of sodium acetate trihydrate in thermal heat storage cycles, Sol. Energy. 46
472 (1991) 97–100.

473 [16] B. Sandnes, J. Rekstad, Supercooling salt hydrates: Stored enthalpy as a function of temperature, Sol. Energy.
474 80 (2006) 616–625. doi:10.1016/j.solener.2004.11.014.

475 [17] M. Dannemand, J.M. Schultz, J.B. Johansen, S. Furbo, Long term thermal energy storage with stable
476 supercooled sodium acetate trihydrate, Appl. Therm. Eng. 91 (2015) 671–678.
477 doi:10.1016/j.applthermaleng.2015.08.055.

478 [18] M. Dannemand, W. Kong, J. Fan, J.B. Johansen, S. Furbo, Laboratory Test of a Prototype Heat Storage
479 Module Based on Stable Supercooling of Sodium Acetate Trihydrate, in: Energy Procedia, Elsevier B.V., 2015:
480 pp. 172–181. doi:10.1016/j.egypro.2015.02.113.

481 [19] P. Hu, D.-J. Lu, X.-Y. Fan, X. Zhou, Z.-S. Chen, Phase change performance of sodium acetate trihydrate with
482 AlN nanoparticles and CMC., Sol. Energy Mater. Sol. Cells. 95 (2011) 2645–2649.
483 doi:10.1016/j.solmat.2011.05.025.

484 [20] B.M.L. Garay Ramirez, C. Glorieux, E.S. Martin Martinez, J.J. a Flores Cuautle, Tuning of thermal properties of
485 sodium acetate trihydrate by blending with polymer and silver nanoparticles, Appl. Therm. Eng. 61 (2013)
486 838–844. doi:10.1016/j.applthermaleng.2013.09.049.

487 [21] M. Dannemand, J.B. Johansen, S. Furbo, Solidification Behaviour and Thermal Conductivity of Bulk Sodium
488 Acetate Trihydrate Mixtures with Thickening Agents and Graphite Powder, Sol. Energy Mater. Sol. Cells.

(2015). doi:10.1016/j.solmat.2015.10.038.

[22] H.K. Shin, M. Park, H.-Y. Kim, S.-J. Park, Thermal property and latent heat energy storage behavior of sodium acetate trihydrate composites containing expanded graphite and carboxymethyl cellulose for phase change materials, Appl. Therm. Eng. 75 (2015) 978–983. doi:10.1016/j.applthermaleng.2014.10.035.

[23] B. Zalba, J.M. Marin, L.F. Cabeza, H. Mehling, Review on thermal energy storage with phase change: materials, heat transfer analysis and applications, Appl. Therm. Eng. 23 (2003) 251–283.

[24] M.A. Rogerson, S.S.S. Cardoso, Solidification in heat packs: I. Nucleation rate, AICHE J. 49 (2003) 505–515. doi:10.1002/aic.690490220.

[25] H. Kimura, J. Kai, Phase change stability of sodium acetate trihydrate and its mixtures, Sol. Energy. 35 (1985) 527–534. doi:10.1016/0038-092X(85)90121-5.

[26] S. Furbo, S. Svendsen, Report on heat storage in a solar heating system using salt hydrates, Therm. Insul. Labotatory, DTU, Kgs. Lyngby, Denmark, Rep. 70. (1977).

[27] S. Furbo, Investigations of Heat Storages with salt hydrate as storage medium based on the extra water principle, Therm. Insul. Labotatory, DTU, Kgs. Lyngby, Denmark, Rep. 80. Meddelelse (1978).

[28] N. Araki, M. Futamura, A. Makino, H. Shibata, Measurements of Thermophysical Properties of Sodium Acetate Hydrate, Internaltional J. Thermophys. 16 (1995) 1455–1466.

[29] L.F. Cabeza, J. Roca, M. Nogués, H. Mehling, S. Hiebler, Immersion corrosion tests on metal-salt hydrate pairs used for latent heat storage in the 48 to 58 8C temperature range, Mater. Corros. 53 (2002) 902–907.

[30] P. Moreno, L. Miró, A. Solé, C. Barreneche, C. Solé, I. Martorell, et al., Corrosion of metal and metal alloy containers in contact with phase change materials (PCM) for potential heating and cooling applications, Appl. Energy. 125 (2014) 238–245. doi:10.1016/j.apenergy.2014.03.022.

[31] M.A. Rogerson, S.S.S. Cardoso, Solidification in Heat Packs : III . Metallic Trigger, AIChE J. 49 (2003) 522–529.

[32] S. Furbo, J. Fan, Heat Storage based on a NaCH3COO Water Mixture for Solar Heating Systems, DTU Civil Engineering, Report SR-12-10 (UK), Kgs. Lyngby, Denmark, 2012.

[33] L. Wei, K. Ohsasa, Supercooling and Solidification Behavior of Phase Change, ISIJ Int. 50 (2010) 1265–1269.

[34] Y.A. Cengel, Heat Transfer: A Practical Approach, 2nd ed., McGraw-Hill, 2003.

[35] S. Furbo, Heat Storage for Solar Heating Systems, Educational Note, ISSN 1396-4046, BYG.DTU, Kgs. Lyngby, Denmark, 2005.

[36] X. Sun, Q. Zhang, M. a. Medina, K.O. Lee, Experimental observations on the heat transfer enhancement caused by natural convection during melting of solid–liquid phase change materials (PCMs), Appl. Energy. 162 (2015) 1453–1461. doi:10.1016/j.apenergy.2015.03.078.

[37] V. Weitbrecht, D. Lehmann, A. Richter, Flow distribution in solar collectors with laminar flow conditions, Sol. Energy. 73 (2002) 433–441. doi:10.1016/S0038–092X(03)00006–9.